Ultrasound Obstet Gynecol 2017; **50**: 476–491
Published online 14 August 2017 in Wiley Online Library (wileyonlinelibrary.com). **DOI:** 10.1002/uog.17522.

Color and power Doppler combined with Fetal Intelligent Navigation Echocardiography (FINE) to evaluate the fetal heart

L. YEO[1,2,3] and R. ROMERO[1,4,5,6]

[1]*Perinatology Research Branch, Program for Perinatal Research and Obstetrics, Division of Intramural Research, Eunice Kennedy Shriver National Institute of Child Health and Human Development, NIH, Bethesda, MD and Detroit, MI, USA;* [2]*Detroit Medical Center, Hutzel Women's Hospital, Detroit, MI, USA;* [3]*Department of Obstetrics and Gynecology, Wayne State University School of Medicine, Detroit, MI, USA;* [4]*Department of Obstetrics and Gynecology, University of Michigan, Ann Arbor, MI, USA;* [5]*Department of Epidemiology and Biostatistics, Michigan State University, East Lansing, MI, USA;* [6]*Center for Molecular Medicine and Genetics, Wayne State University, Detroit, MI, USA*

KEYWORDS: 4D; 5D heart color; cardiac; congenital heart disease; fetal echocardiography; spatiotemporal image correlation; STIC; ultrasound

ABSTRACT

Objective *To evaluate the performance of color and bidirectional power Doppler ultrasound combined with Fetal Intelligent Navigation Echocardiography (FINE) in examining the fetal heart.*

Methods *A prospective cohort study was conducted of fetuses in the second and third trimesters with a normal heart or with congenital heart disease (CHD). One or more spatiotemporal image correlation (STIC) volume datasets, combined with color or bidirectional power Doppler (S-flow) imaging, were acquired in the apical four-chamber view. Each successfully obtained STIC volume was evaluated by STICLoop™ to determine its appropriateness before applying the FINE method. Visualization rates for standard fetal echocardiography views using diagnostic planes and/or Virtual Intelligent Sonographer Assistance (VIS-Assistance®) were calculated for grayscale (removal of Doppler signal), color Doppler and S-flow Doppler. In four cases with CHD (one case each of tetralogy of Fallot, hypoplastic left heart and coarctation of the aorta, interrupted inferior vena cava with azygos vein continuation and asplenia, and coarctation of the aorta with tricuspid regurgitation and hydrops), the diagnostic potential of this new technology was presented.*

Results *A total of 169 STIC volume datasets of the normal fetal heart (color Doppler,* n = *78; S-flow Doppler,* n = *91) were obtained from 37 patients. Only a single STIC volume of color Doppler and/or a single volume of S-flow Doppler per patient were analyzed using FINE. Therefore, 60 STIC volumes (color Doppler,* n = *27; S-flow Doppler,* n = *33) comprised the final study group. Median gestational age at sonographic examination was 23 (interquartile range, 21–27.5) weeks. Color Doppler FINE generated nine fetal echocardiography views (grayscale) using (1) diagnostic planes in 73–100% of cases, (2) VIS-Assistance in 100% of cases, and (3) a combination of diagnostic planes and/or VIS-Assistance in 100% of cases. The rate of generating successfully eight fetal echocardiography views with appropriate color and S-flow Doppler information was 89–100% and 91–100% of cases, respectively, using a combination of diagnostic planes and/or VIS-Assistance. However, the success rate for the ninth echocardiography view (i.e. superior and inferior venae cavae) was 33% and 30% for color and S-flow Doppler, respectively. In all four cases of CHD, color Doppler FINE demonstrated evidence of abnormal fetal cardiac anatomy and/or hemodynamic flow.*

Conclusions *The FINE method applied to STIC volumes of normal fetal hearts acquired with color or bidirectional power Doppler information can generate successfully eight to nine standard fetal echocardiography views (via grayscale, color Doppler or power Doppler) in the second and third trimesters. In cases of CHD, color Doppler FINE demonstrates successfully abnormal anatomy and/or Doppler flow characteristics. Published 2017. This article is a U.S. Government work and is in the public domain in the USA. Ultrasound in Obstetrics & Gynecology published by John Wiley & Sons Ltd on behalf of the International Society of Ultrasound in Obstetrics and Gynecology.*

Correspondence to: Dr L. Yeo and Dr R. Romero, Perinatology Research Branch, NICHD, NIH, DHHS, Hutzel Women's Hospital, 3990 John R, 4 Brush, Detroit, MI 48201, USA (e-mail: lyeo@med.wayne.edu and prbchiefstaff@med.wayne.edu)

Accepted: 3 March 2017

ORIGINAL PAPER

INTRODUCTION

Color Doppler flow mapping is the real-time display of two-dimensional (2D) flow patterns superimposed on cross-sectional pulse echo images of anatomical structures[1–4]. This modality is a valuable and integral component of fetal cardiac examination[5–8], since it allows identification of cardiac structures and vasculature[9–11] and the pattern and direction of blood flow throughout the heart[12–16], and directs spectral Doppler interrogation of the fetal circulation (e.g. ductus venosus)[17,18]. Indeed, some investigators have recommended that color Doppler should be employed routinely in fetal cardiac screening[6,18,19].

In fetuses with congenital heart disease (CHD), color Doppler sonography is essential to identify and characterize abnormal cardiovascular anatomy, flow patterns/disturbances and cardiac function[16,17,20–24]. Both the accuracy and prenatal detection of CHD improve by applying color Doppler flow mapping, especially in the presence of complex cardiac defects[24–26].

In contrast to color Doppler sonography, power Doppler analyzes the intensity or amplitude of Doppler signals, instead of their frequency shift[27]. When Doppler frequency shifts are then combined with signal amplitude, there is digital broadband assessment of Doppler signals, with resulting high-definition (HD) flow[28]. Such modality is superior to conventional color Doppler sonography, since it demonstrates higher sensitivity in depicting small vessels and low flow patterns, higher resolution, and good lateral discrimination[28,29].

All color Doppler modalities (i.e. color Doppler[19,30–58], power Doppler[33,34,43,45,46,51,52,56,57,59,60], and HD flow Doppler[43,46,53,61]) can be combined with four-dimensional (4D) ultrasound and spatiotemporal image correlation (STIC) to assess fetal cardiac flow and anatomical relationships in both normal fetuses[32–35,44,47–51,58,60,61] and those with CHD[30,31,36–38,40,42–45,48,52–56,59]. Recently, a new method known as Fetal Intelligent Navigation Echocardiography (FINE) was developed, which automatically generates and displays nine standard fetal echocardiography views in normal hearts by applying 'intelligent navigation' technology to STIC volume datasets[62]. Thus far, only STIC volumes obtained via grayscale ultrasound could be analyzed using the FINE method[62–64]. However, a recent technological advance now allows STIC volumes to be acquired in combination with color or bidirectional power Doppler information, so that fetal echocardiography views generated by FINE can be displayed with either modality. Therefore, we conducted this prospective study to describe, for the first time, the clinical feasibility of using color Doppler FINE to evaluate fetuses with normal hearts, as well as those with CHD.

METHODS

Subjects

Forty-one pregnant women having a singleton fetus with a normal heart or CHD in the second or third trimesters were approached prospectively to undergo STIC volume acquisition combined with color or bidirectional power Doppler. This was a sample size of convenience. Patients were examined at the Detroit Medical Center/Wayne State University and the Perinatology Research Branch of NICHD, NIH, DHHS. All women were enrolled in research protocols approved by the Institutional Review Board of NICHD, NIH, and by the Human Investigation Committee of Wayne State University. All participants provided written informed consent for the use of sonographic images for research purposes.

Acquisition of spatiotemporal image correlation (STIC) volumes

Since its original invention[62], the FINE method has been integrated into an ultrasound platform (UGEO WS80A; Samsung Healthcare, Seoul, Korea) and is known as 5D Heart technology. When such technology is used to acquire STIC volume datasets of the fetal heart in combination with color or bidirectional power Doppler (known as S-flow), this is called 5D Heart Color (or color Doppler FINE). S-flow is a highly sensitive Doppler technology utilizing both phase (directional) and amplitude (intensity) data to ensure vascular documentation. In the context of this work, the term 'color Doppler FINE' refers to both color and S-flow Doppler modalities.

STIC technology allows acquisition of a volume dataset of the fetal heart and displays a cineloop of a complete single cardiac cycle in motion[65–70]. The image quality of a given STIC volume dataset can be improved substantially by optimizing both the grayscale and color Doppler settings before volume acquisition[39]. Moreover, improper color and power Doppler settings may lead to both false-positive and false-negative diagnoses. The quality of a given STIC volume also depends upon the frame rate of the image[68]. Therefore, on 2D imaging, we first maximized the frame rate by decreasing the depth on the monitor display, narrowing the sector width, magnifying the image and placing a single focal zone at, or below, the level of the fetal heart.

Next, the fetal heart was interrogated with color or S-flow Doppler ultrasound (see Appendix S1 for Doppler settings). In an apical four-chamber view, the color box was kept as small as possible around the entire fetal chest circumference, since this action has the greatest impact on frame rate[5,71]. For each fetus, modifications were made to the color gain and velocity scale (or pulse repetition frequency; PRF) to display flow across valves and vessels, with the goal of keeping the frame rate as high as possible (frame rates ranged from 15 to 31 Hz and 15 to 28 Hz for color Doppler and S-flow Doppler STIC volumes, respectively). This included adjustments so that (1) there was homogeneous color display across valves and vessels without aliasing; (2) the color signal filled the lumen of the great vessels and there was clear definition of vascular contour; and (3) there was no amplification of noise and artifacts. A high velocity scale was used intentionally to allow color Doppler interrogation of the atrioventricular valves,

as well as the great vessels and semilunar valves[6,28]. Lower velocity ranges can lead to inappropriate color aliasing, as well as false-positive diagnoses of turbulence or abnormal flow dynamics[6]. However, we recognized that by using a high PRF, this would lead to reduced sensitivity, such that low velocity flow (e.g. caval or pulmonary veins) might not be identified through color Doppler FINE.

5D Heart technology was activated, and its settings adjusted to the following: scan quality (high) and scan line ratio as quality (0.1). The 'region of interest' box to acquire STIC volumes was adjusted to encompass the entire fetal chest circumference, so that all cardiac anatomical information would be contained[68]. Patients were asked to momentarily suspend breathing during the volume acquisition. STIC volume datasets were acquired from an apical four-chamber view using a motorized curved-array transducer (CV1-8A) by automatic transverse sweeps through the fetal chest. The apical four-chamber view was chosen as the acquisition plane, since optimal color Doppler information is obtained in transverse planes by using an insonation angle that is either parallel to the direction of blood flow or nearly so[6,18,54]. When cardiac structures are oriented perpendicular to the transducer beam (e.g. subcostal four-chamber view), Doppler frequency shifts are significantly attenuated. An attempt was made to acquire one or more STIC volume datasets per patient only if the following criteria were met: (1) adequate image quality; (2) fetal spine located between the 5- and 7-o'clock position; (3) minimal or absent shadowing (including a clearly visible transverse aortic arch); and (4) absent fetal breathing, hiccups or movement[63]. Acquisition times ranged from 10 to 12 s, depending on fetal motion, and the acquisition angle ranged between 20° and 45°, depending on gestational age. All STIC volumes were saved onto the hard drive of the ultrasound machine for analysis.

STICLoop evaluation

Although multiple STIC volume datasets were acquired in the course of a given scanning session, only a maximum of two volumes per patient (one acquired with color Doppler and one with S-flow Doppler imaging) were included in the study. Such volumes were selected for analysis by color Doppler FINE only if determined to be appropriate using STICLoop™ criteria (see Appendix S1 for criteria and an explanation about STICLoop)[62–64,68]. It is noteworthy that, when STIC volumes are obtained in combination with color or S-flow Doppler ultrasound, Doppler information is not depicted in the scrolling transverse planes of the cineloop (Videoclip S1). This is done intentionally to allow the sonologist to evaluate accurately the STICLoop criteria. One exception is the last criterion, in which color or power Doppler information is depicted in the sagittal plane (Videoclip S1). However, the sonologist has the option to manually turn off the color signal, so that the sagittal plane can be evaluated for motion artifacts.

Analysis of STIC volume datasets by color Doppler FINE technology

Marking fetal cardiac structures

Seven anatomical structures of the fetal heart (see Appendix S1 for further details) were marked on the screen to generate an internal geometrical model of the fetal heart[62,63,70]. After marking is completed, nine standard fetal echocardiography views are automatically generated and displayed by FINE, as diagnostic planes and/or Virtual Intelligent Sonographer Assistance (VIS-Assistance®)[62–64,70]. It is noteworthy that during the marking process itself, color or power Doppler information is intentionally not displayed to facilitate ease of marking.

Fetal echocardiography views

After the marking process is completed, nine fetal echocardiography views are automatically generated[62–64]: (1) four chamber; (2) five chamber; (3) left ventricular outflow tract; (4) short-axis view of great vessels/right ventricular outflow tract; (5) three vessels and trachea (3VT); (6) abdomen/stomach; (7) ductal arch; (8) aortic arch; and (9) superior and inferior venae cavae. Fetal echocardiography views are displayed simultaneously in a single template as nine *diagnostic planes* and contain either color Doppler (Figure 1 and Videoclip S2) or bidirectional power Doppler (S-flow) (Figure 2 and Videoclip S3) information, depending on the type of STIC volume acquisition. However, color Doppler FINE allows the option of turning off the color display, so that only grayscale information is depicted (Figure 3 and Videoclip S4).

Color Virtual Intelligent Sonographer Assistance (VIS-Assistance)

Similarly to the original FINE method, VIS-Assistance may also be activated in color Doppler FINE for each of the nine cardiac diagnostic planes, and is known as color VIS-Assistance. The purpose is to (1) improve the success of obtaining the fetal echocardiography view of interest in grayscale (by doing so, an appropriate Doppler signal becomes visible; Videoclip S5); and (2) allow operator-independent sonographic navigation and exploration of surrounding structures in the diagnostic plane[62,63,70]. The VIS-Assistance tool essentially functions as a virtual sonographer that 'scans' the STIC volume in a targeted manner (as a videoclip) to allow the complexity of the fetal heart to be studied in further detail[62,63,70].

Evaluation of fetal echocardiography views with grayscale, color Doppler or S-flow Doppler information

Using color Doppler FINE, we evaluated a given STIC volume dataset of the normal fetal heart in the following ways: (1) grayscale only (Figure 3): we calculated the frequency of generating nine fetal echocardiography

Ultrasound in Obstetrics & Gynecology published by John Wiley & Sons Ltd on behalf of the International Society of Ultrasound in Obstetrics and Gynecology.

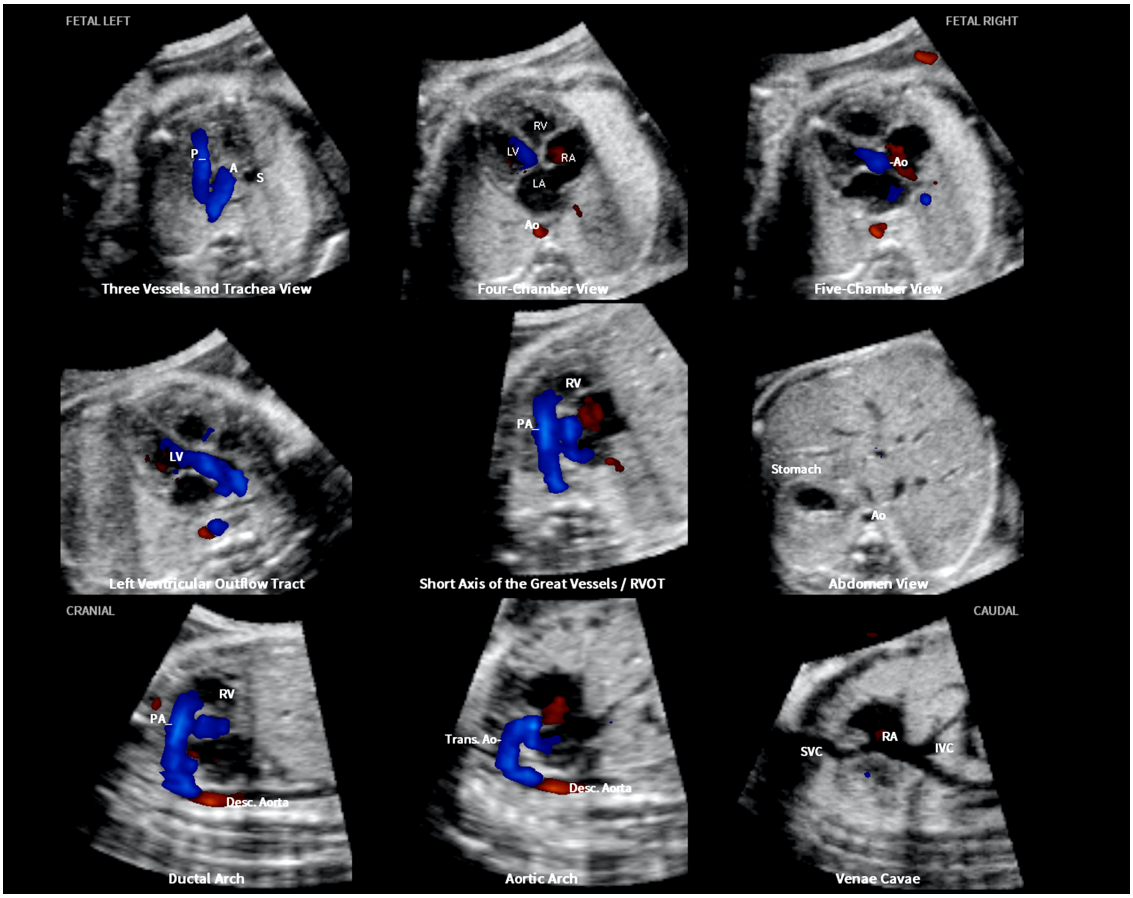

Figure 1 Color Doppler spatiotemporal image correlation volume dataset of normal fetal heart, showing nine cardiac diagnostic planes displayed automatically in single template through color Doppler Fetal Intelligent Navigation Echocardiography (see Videoclip S2). Color Doppler signals are displayed in systole. The unique feature of automatic labeling (through intelligent navigation) of each plane, anatomical structures, fetal left and right sides and cranial and caudal ends is shown. Labeling is distinctive because it stays with corresponding anatomical structures, even as image is increased in size (zoom). A, transverse aortic arch; Ao, aorta; Desc., descending; IVC, inferior vena cava; LA, left atrium; LV, left ventricle; P, pulmonary artery; PA, pulmonary artery; RA, right atrium; RV, right ventricle; RVOT, right ventricular outflow tract; S, superior vena cava; SVC, superior vena cava; Trans., transverse.

views using (a) diagnostic planes only, (b) VIS-Assistance only, and (c) a combination of diagnostic planes and/or VIS-Assistance[62–64]; (2) color Doppler only (Figure 1): we calculated the frequency of depicting appropriate color Doppler information using a combination of diagnostic planes and/or VIS-Assistance; and (3) S-flow Doppler only (Figure 2): we calculated the frequency of depicting appropriate bidirectional power Doppler information using a combination of diagnostic planes and/or VIS-Assistance. When evaluating fetal echocardiography views using grayscale only, we arbitrarily evaluated the color Doppler STIC volume, in which we turned off the color display so that only grayscale information was depicted. However, for fetuses in which a color Doppler STIC volume was not available, we evaluated views in grayscale by turning off the color display in S-flow STIC volumes.

In addition, for four cardiac VIS-Assistance views (grayscale only), we prespecified that certain anatomical structures should also be visualized in order to consider the VIS-Assistance as being successful in depicting the echocardiography view (see Appendix S1)[62–64,72]. An advantage of the four-chamber view VIS-Assistance is that it allows automatic visualization of the atrial septum (both septum primum and septum secundum) and pulmonary veins in grayscale[62,63]. Therefore, for the four-chamber view VIS-Assistance (grayscale only), we recorded how frequently the atrial septum and pulmonary veins could be visualized when compared with the four-chamber view diagnostic plane.

For color or S-flow Doppler STIC volume datasets of normal fetal hearts, we determined the success rate of color Doppler FINE to generate nine echocardiography views with appropriate Doppler information by first evaluating the diagnostic planes for the criteria listed in Table 1[6,73]. Color VIS-Assistance videoclips were only reviewed if the diagnostic plane was unsuccessful in meeting such criteria. When evaluating the fetal echocardiography views generated by color Doppler FINE, post-processing adjustments in image quality[33] were performed as necessary, including the following settings: (1) color threshold and balance; and (2) brightness, midtones and contrast. Refer to Appendix S1 for 5D Heart Color settings and information on color threshold and balance.

For a given fetus, only one or two STIC volume datasets combined with color and/or S-flow Doppler information

Ultrasound in Obstetrics & Gynecology published by John Wiley & Sons Ltd on behalf of the International Society of Ultrasound in Obstetrics and Gynecology.

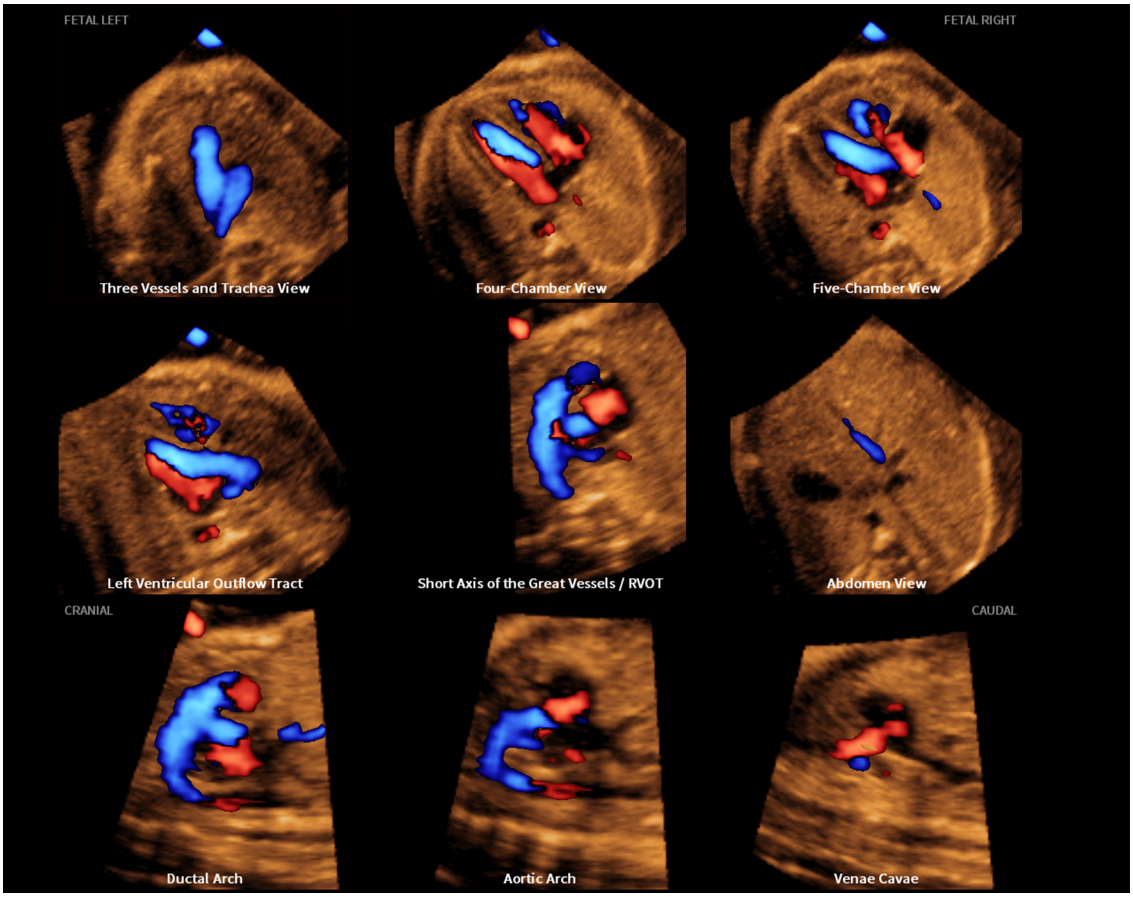

Figure 2 S-flow Doppler (bidirectional power Doppler) spatiotemporal image correlation volume dataset of normal fetal heart, showing nine cardiac diagnostic planes displayed automatically in single template through color Doppler Fetal Intelligent Navigation Echocardiography (see Videoclip S3). Both diastolic and systolic flow is demonstrated at the same time in echocardiography views.

were analyzed for the study. However, for such a fetus, the nine echocardiography views were evaluated either twice (e.g. grayscale only with Doppler information turned off and then Doppler only) or three times (e.g. grayscale only with Doppler information turned off, color Doppler only and S-flow Doppler only), depending upon the type of STIC volume dataset that had been acquired.

Finally, for each STIC volume dataset (grayscale only, color Doppler only, S-flow Doppler only), we also calculated[62–64] (1) the maximum number of fetal echocardiography views that were obtained successfully through diagnostic planes and/or VIS-Assistance; and (2) the success rate of obtaining four specific fetal echocardiography views (four chamber; left ventricular outflow tract; short-axis view of great vessels/right ventricular outflow tract; and abdomen/stomach) through diagnostic planes and/or VIS-Assistance.

Fetuses with congenital heart defects

In four fetuses with CHD (confirmed by fetal/postnatal echocardiography or surgery), we tested color Doppler FINE to determine whether (1) abnormal cardiac anatomy could be identified (grayscale only); and (2) color/S-flow Doppler provided additional information to that obtained on grayscale alone.

Other clinical applications of color Doppler FINE

Finally, we recorded clinical applications of color Doppler FINE that were noted during the analysis of color or S-flow Doppler STIC volumes. Such information was recorded if it was thought to be of diagnostic potential.

RESULTS

STIC volumes

A total of 169 STIC volume datasets of normal fetal hearts were acquired using color Doppler ($n = 78$) and S-flow Doppler ($n = 91$) imaging in 37 women undergoing ultrasound examination. The number of volumes obtained per patient was: one, $n = 6$; two, $n = 6$; three, $n = 5$; four, $n = 3$; five, $n = 6$; six, $n = 1$; seven, $n = 8$; nine, $n = 2$; and fourteen, $n = 1$. All STIC volumes were saved onto the hard drive of the ultrasound machine and then evaluated by STICLoop. From the volumes determined to be appropriate, only a single volume of color Doppler and/or a single volume of S-flow Doppler per patient was selected for analysis using color Doppler FINE. When multiple appropriate STIC volumes were available per fetus, the volume dataset considered to be of highest quality was chosen. Therefore, 60 STIC volume datasets (color

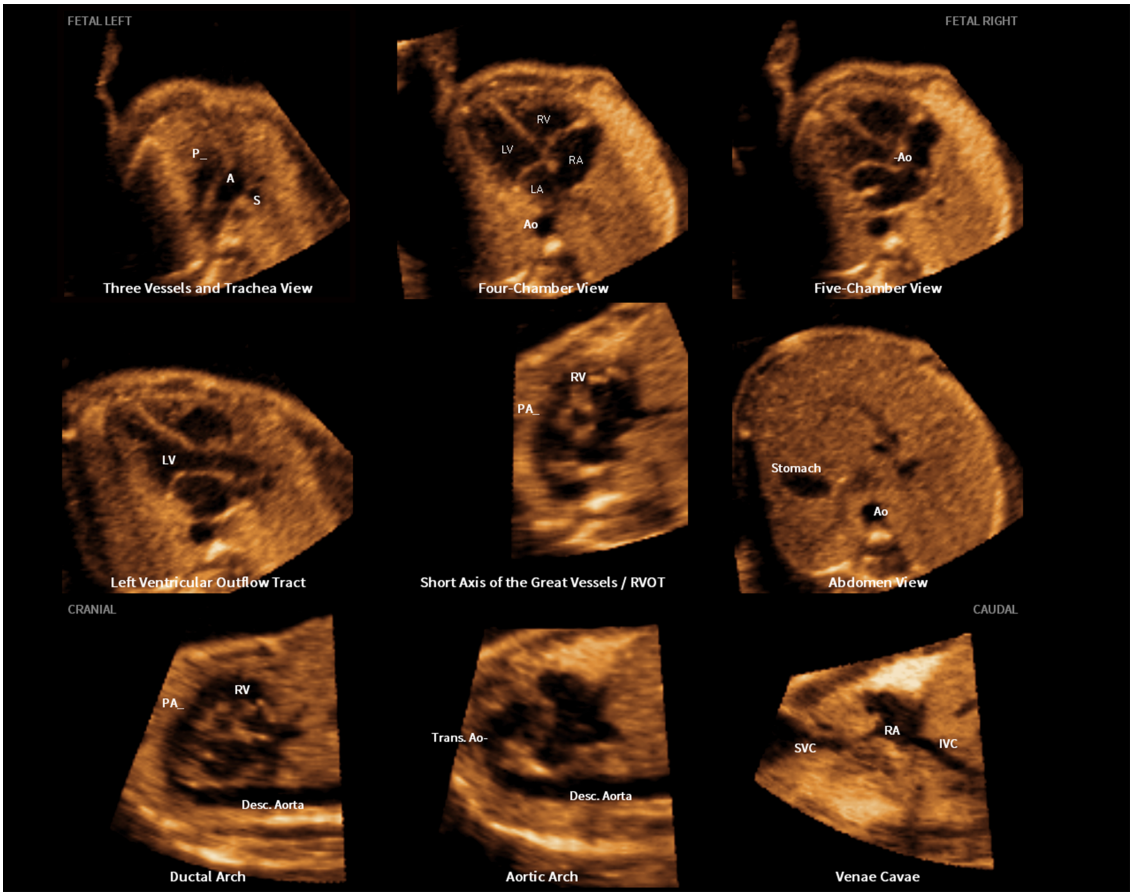

Figure 3 Spatiotemporal image correlation volume dataset of normal fetal heart acquired with color Doppler imaging and analyzed by color Doppler Fetal Intelligent Navigation Echocardiography (see Videoclip S4). Color display is turned off so that only grayscale information is depicted in nine cardiac diagnostic planes. The unique feature of automatic labeling (through intelligent navigation) of each plane, anatomical structures, fetal left and right sides and cranial and caudal ends is shown. A, transverse aortic arch; Ao, aorta; Desc., descending; IVC, inferior vena cava; LA, left atrium; LV, left ventricle; P, pulmonary artery; PA, pulmonary artery; RA, right atrium; RV, right ventricle; RVOT, right ventricular outflow tract; S, superior vena cava; SVC, superior vena cava; Trans., transverse.

Doppler, $n = 27$; S-flow Doppler, $n = 33$) of 37 fetuses with normal hearts comprised the final study group. The median gestational age at the sonographic examination was 23 (interquartile range, 21–27.5) weeks, with 27% (10/37) of fetuses being in the third trimester. Nineteen percent (7/37) of fetuses were in breech presentation so that the cardiac apex was originally pointing to the right side of the ultrasound monitor screen.

Performance of color Doppler FINE to generate fetal echocardiography views

All 60 STIC volume datasets combined with Doppler were analyzed using color Doppler FINE. Testing consisted of evaluating the following: (1) grayscale only: 333 diagnostic planes (37 STIC volumes × 9) and 333 VIS-Assistance videoclips (37 STIC volumes × 9); (2) color Doppler only: 243 diagnostic planes (27 STIC volumes × 9) and 99 VIS-Assistance videoclips; and (3) S-flow Doppler only: 297 diagnostic planes (33 STIC volumes × 9) and 113 VIS-Assistance videoclips. Therefore, we evaluated a total of 873 diagnostic planes and 545 VIS-Assistance videoclips, for a total of 1418 images.

Visualization rates for fetal echocardiography views in grayscale

After color Doppler FINE generated nine fetal echocardiography views, we analyzed all images in grayscale by turning off either color or S-flow Doppler information. Analysis in grayscale was performed for 37 STIC volumes (color Doppler, $n = 27$; S-flow Doppler, $n = 10$). Color Doppler FINE was able to generate fetal echocardiography views using (1) diagnostic planes in 73–100% of cases; (2) VIS-Assistance in 100% of cases; and (3) a combination of diagnostic planes and/or VIS-Assistance in 100% of cases (Table 2). An example of nine cardiac diagnostic planes in a single template with the additional feature of automatic labeling through intelligent navigation technology is shown in Figure 3[62–64,70]. Through the FINE method, automatic labeling of anatomical structures (atrial and ventricular chambers, great vessels, venae cavae and stomach) within diagnostic planes is possible because the system 'infers' the actual location of structures in space[70]. In addition, automatic labeling of fetal orientation (e.g. left, right, cranial, caudal) and naming of each fetal echocardiography view (i.e. diagnostic planes) occurs[62–64,70]. Automatic

Table 1 Criteria to evaluate whether fetal echocardiography views generated by color Doppler Fetal Intelligent Navigation Echocardiography (FINE) of color or S-flow Doppler spatiotemporal image correlation volume datasets of normal fetal hearts contain appropriate Doppler information

Fetal echocardiography view generated by color Doppler FINE	*Criteria for appropriate Doppler information*
Four chamber	Diastolic perfusion across atrioventricular valves (two separate and equal color stripes), with no evidence of valve regurgitation during systole No color flow observed crossing ventricular septum
Five chamber	Systolic perfusion in aortic root emerging from left ventricle Aortic valve closed and non-regurgitant in diastole
Left ventricular outflow tract	Systolic perfusion across aortic valve without retrograde flow
Short-axis view of great vessels/ right ventricular outflow tract	Systolic perfusion across pulmonary valve, trunk, ductus arteriosus and right pulmonary artery without retrograde flow Diastolic perfusion through tricuspid valve
Three vessels and trachea	Systolic perfusion through pulmonary trunk and ductus arteriosus, as well as transverse aortic arch and isthmus (antegrade and equal flow in both great vessels) Ductal and aortic arches positioned to left of trachea and spine, forming V-configuration as they join descending aorta Color flow within superior vena cava may or may not be depicted
Abdomen/stomach	Stomach on left side of abdomen Transverse section of descending aorta in front and to left of spine Liver visualized Flow within descending aorta and inferior vena cava may or may not be depicted
Ductal arch	Systolic perfusion through pulmonary trunk and ductus arteriosus Flow within descending aorta may or may not be depicted
Aortic arch	Systolic perfusion through ascending aorta and transverse aortic arch Flow within descending aorta may or may not be depicted
Superior and inferior venae cavae	Blood flow in superior and inferior venae cavae towards right atrium

labeling may be activated for all modalities: grayscale (Videoclip S4), color Doppler (Videoclip S2), and S-flow Doppler (Videoclip S3).

Visualization rates for fetal echocardiography views in color or S-flow Doppler

A total of 27 STIC volumes acquired with color Doppler information were analyzed using color Doppler FINE. The success rate of obtaining eight fetal echocardiography views with appropriate color Doppler information was 89–100% using a combination of diagnostic planes and/or VIS-Assistance (Table 3). However, for the ninth view (visualization of the superior and inferior venae cavae), the success rate was (1) 85% for superior vena cava only ($n = 23$); (2) 33% for inferior vena cava only ($n = 9$); and (3) 33% for both superior and inferior venae cavae ($n = 9$) (Table 3).

There were 33 STIC volumes acquired with S-flow Doppler information that were analyzed using color Doppler FINE. The success rate of obtaining eight fetal echocardiography views with appropriate S-flow Doppler information was 91–100% using a combination of diagnostic planes and/or VIS-Assistance (Table 4). However, for the ninth view (visualization of the superior and inferior venae cavae), the success rate was (1) 79% for superior vena cava only ($n = 26$); (2) 33% for inferior vena cava only ($n = 11$); and (3) 30% for both superior and inferior venae cavae ($n = 10$) (Table 4).

Observations about diagnostic planes and VIS-Assistance in fetuses with normal hearts

The maximum number of fetal echocardiography views (grayscale information) obtained successfully through diagnostic planes or VIS-Assistance for each STIC volume dataset of normal hearts ($n = 37$) is reported in Table 5. For diagnostic planes, 83.5% ($n = 31$) of STIC volumes demonstrated either eight (40.5%; $n = 15$) or all nine (43.0%; $n = 16$) echocardiography views, while 13.5% ($n = 5$) demonstrated seven views. For VIS-Assistance, 100% (37/37) of STIC volumes demonstrated all nine echocardiography views.

For each color ($n = 27$) or S-flow Doppler ($n = 33$) STIC volume dataset of normal fetal hearts, the maximum number of fetal echocardiography views obtained successfully through diagnostic planes and/or VIS-Assistance was (1) color Doppler volumes: 93% ($n = 25$) demonstrated either eight (63%; $n = 17$) or all nine (30%; $n = 8$) echocardiography views, while 3.5% ($n = 1$) demonstrated seven views and 3.5% ($n = 1$) demonstrated six views; (2) S-flow Doppler volumes: 94% ($n = 31$) demonstrated either eight (67%; $n = 22$) or all nine (27%; $n = 9$) echocardiography views, while 6% ($n = 2$) demonstrated seven views.

The success rates of obtaining the four chamber, left ventricular outflow tract, short-axis view of great vessels/right ventricular outflow tract and abdomen/stomach views for each STIC volume dataset of normal hearts

Table 2 Color Doppler Fetal Intelligent Navigation Echocardiography (grayscale information only): success rates of obtaining nine fetal echocardiography views after applying intelligent navigation to 37 normal spatiotemporal image correlation volume datasets using diagnostic planes and/or Virtual Intelligent Sonographer Assistance (VIS-Assistance)

	Diagnostic plane (n = *37*)		*VIS-Assistance* (n = *37*)		*Diagnostic plane and/or VIS-Assistance* (n = *37*)	
Fetal echocardiography view	n *(%)*	*95% CI (%)*	n *(%)*	*95% CI (%)*	n *(%)*	*95% CI (%)*
1. Four chamber	37 (100)	89–100	37 (100)	89–100	37 (100)	89–100
2. Five chamber	36 (97)	85– > 99.9	37 (100)	89–100	37 (100)	89–100
3. LVOT	32 (86)	72–95	37 (100)	89–100	37 (100)	89–100
4. Short-axis view of great vessels/RVOT	33 (89)	75–96	37 (100)	89–100	37 (100)	89–100
5. 3VT	36 (97)	85– > 99.9	37 (100)	89–100	37 (100)	89–100
6. Abdomen/stomach	37 (100)*	89–100	37 (100)†	89–100	37 (100)	89–100
7. Ductal arch	29 (78)	63–89	37 (100)	89–100	37 (100)	89–100
8. Aortic arch	37 (100)	89–100	37 (100)	89–100	37 (100)	89–100
9. SVC and IVC	27 (73)	57–85	37 (100)	89–100	37 (100)	89–100
SVC	34 (92)	78–98	—	—	—	—
IVC	30 (81)	65–91	—	—	—	—

Wald method used to calculate two-sided CIs for proportions; as true proportion cannot exceed 100%, upper CIs were truncated at 100%. *Defined as visualization of stomach in diagnostic plane. †Defined as visualization of both stomach and four-chamber view in VIS-Assistance (to determine situs). 3VT, three vessels and trachea; IVC, inferior vena cava; LVOT, left ventricular outflow tract; RVOT, right ventricular outflow tract; SVC, superior vena cava.

Table 3 Color Doppler Fetal Intelligent Navigation Echocardiography (color Doppler information only): success rates of obtaining nine fetal echocardiography views with appropriate color Doppler information after applying intelligent navigation to 27 normal spatiotemporal image correlation (STIC) volume datasets using a combination of diagnostic planes and/or Virtual Intelligent Sonographer Assistance (VIS-Assistance)

	Diagnostic plane and/or VIS-Assistance (n = *27*)	
Fetal echocardiography view	n *(%)*	*95% CI (%)*
1. Four chamber	27 (100)	85–100
2. Five chamber	24 (89)	71–97
3. LVOT	26 (96)	80– > 99.9
4. Short-axis view of great vessels/RVOT	27 (100)	85–100
5. 3VT*	27 (100)	85–100
6. Abdomen/stomach†	27 (100)	85–100
7. Ductal arch‡	27 (100)	85–100
8. Aortic arch§	27 (100)	85–100
9. SVC and IVC	9 (33)	19–52
SVC	23 (85)	67–95
IVC	9 (33)	19–52

Wald method used to calculate two-sided CIs for proportions; as true proportion cannot exceed 100%, upper CIs were truncated at 100%. *No flow in superior vena cava (SVC) in 74% ($n = 20$) and flow in SVC in 26% ($n = 7$). †No flow in both inferior vena cava (IVC) and descending aorta in 70% ($n = 19$), no flow in descending aorta, but flow in IVC in 22% ($n = 6$), flow in both IVC and descending aorta in 4% ($n = 1$) and flow in descending aorta, but no flow in IVC in 4%; $n = 1$. ‡Flow in descending aorta in 59% ($n = 16$) and no flow in descending aorta in 41% ($n = 11$). §Flow in descending aorta in 56% ($n = 15$) and no flow in descending aorta in 44% ($n = 12$). 3VT, three vessels and trachea; LVOT, left ventricular outflow tract; RVOT, right ventricular outflow tract.

Table 4 Color Doppler Fetal Intelligent Navigation Echocardiography (S-flow Doppler information only): success rates of obtaining nine fetal echocardiography views with appropriate color Doppler information after applying intelligent navigation to 33 normal spatiotemporal image correlation volume datasets using a combination of diagnostic planes and/or Virtual Intelligent Sonographer Assistance (VIS-Assistance)

	Diagnostic plane and/or VIS-Assistance ($n = 33$)	
Fetal echocardiography view	n *(%)*	*95% CI (%)*
1. Four chamber	30 (91)	76–98
2. Five chamber	33 (100)	88–100
3. LVOT	33 (100)	88–100
4. Short-axis view of great vessels/RVOT	33 (100)	88–100
5. 3VT*	33 (100)	88–100
6. Abdomen/Stomach†	33 (100)	88–100
7. Ductal arch‡	33 (100)	88–100
8. Aortic arch§	33 (100)	88–100
9. SVC and IVC	10 (30)	17–48
SVC	26 (79)	62–90
IVC	11 (33)	20–50

Wald method used to calculate two-sided CIs for proportions; as true proportion cannot exceed 100%, upper CIs were truncated at 100%. *No flow in superior vena cava (SVC) in 67% ($n = 22$) and flow in SVC in 33% ($n = 11$). †No flow in both inferior vena cava (IVC) and descending aorta in 58% ($n = 19$), no flow in descending aorta, but flow in IVC in 21% ($n = 7$), flow in descending aorta, but no flow in IVC in 12% ($n = 4$) and flow in both IVC and descending aorta in 9% ($n = 3$). ‡Flow in descending aorta in 64% ($n = 21$) and no flow in descending aorta in 36% ($n = 12$). §Flow in descending aorta in 64% ($n = 21$) and no flow in descending aorta in 36% ($n = 12$). 3VT, three vessels and trachea; LVOT, left ventricular outflow tract; RVOT, right ventricular outflow tract.

were (1) 76% (28/37) using diagnostic planes and 100% (37/37) using VIS-Assistance for grayscale; (2) 96% (26/27) using diagnostic planes and/or VIS-Assistance for color Doppler; and (3) 91% (30/33) using diagnostic planes and/or VIS-Assistance for S-flow Doppler.

For STIC volumes (grayscale information only), we recorded visualization rates of the atrial septum, pulmonary veins and determination of situs. Both the atrial septum primum and septum secundum were seen in 65% (24/37) of cases in the four-chamber view

Table 5 Number of fetal echocardiography views (grayscale information) obtained successfully through diagnostic planes or Virtual Intelligent Sonographer Assistance (VIS-Assistance) for each spatiotemporal image correlation (STIC) volume dataset of normal hearts ($n = 37$)

Number of fetal echocardiography views obtained succesfully (maximum = 9)	*Diagnostic planes (n = 37)*	*VIS-Assistance (n = 37)*
5	1 (3)	—
6	—	—
7	5 (13.5)	—
8	15 (40.5)	—
9	16 (43)	37 (100)
Total	37 (100)	37 (100)

Data are given as *n* (%).

diagnostic plane, but were seen in 100% (37/37) when VIS-Assistance was employed. The pulmonary veins were seen in 46% (17/37) of cases in the four-chamber view diagnostic plane, but were seen in 100% (37/37) of cases when VIS-Assistance was employed. For the abdomen/stomach VIS-Assistance, both the stomach and the four-chamber view were visualized in 100% (37/37) of cases, so that situs could be determined (Table 2).

Color Doppler FINE method in cases of congenital heart defects

In four cases of CHD, we acquired STIC volume datasets combined with color and/or S-flow Doppler imaging for analysis by color Doppler FINE.

Tetralogy of Fallot

The application of S-flow Doppler is illustrated in a 31-week fetus with tetralogy of Fallot (Figure 4, Videoclip S6). Six echocardiography views were abnormal and demonstrated the typical features of this cardiac defect. The 3VT view showed a narrow pulmonary artery due to stenosis, while the transverse aortic arch was prominent. There was a 'Y-shaped' appearance of the great vessels and antegrade flow (blue color) was seen. As is commonly noted in conotruncal abnormalities, the four-chamber view appeared normal, with diastolic perfusion across both atrioventricular valves. Both the five-chamber and left ventricular outflow tract views showed an overriding aorta, dilated aortic root and perimembranous ventricular septal defect. Shunting of blood was seen from the right ventricle across the ventricular septal defect into the aortic root (five-chamber view) and large overriding aorta (left ventricular outflow tract view). In the short-axis view of the great vessels/right ventricular outflow tract, the pulmonary artery was narrow with a small ductus arteriosus and the cross-section of the aorta was dilated. The ductal arch demonstrated similar findings. The S-flow Doppler signal was helpful in delineating the anatomy of the pulmonary artery and ductus arteriosus, as well as confirming antegrade flow in these structures. In the aortic arch view, the aortic root was dilated and there was a prominent ascending aorta.

Hypoplastic left heart and coarctation of the aorta

In a 26-week fetus with hypoplastic left heart and coarctation of the aorta, seven echocardiography views were abnormal and the addition of color Doppler was invaluable in defining the defect (Figure 5, Videoclip S7). The 3VT showed a hypoplastic transverse aortic arch with retrograde flow (red color), along with a dilated pulmonary artery demonstrating antegrade flow (blue color) and aliasing at the ductus arteriosus. In the four-chamber view, the left side of the heart was severely hypoplastic. There was antegrade flow through the tricuspid valve during diastole, but absent flow through the atretic mitral valve. The five-chamber view also demonstrated a severely hypoplastic left side, antegrade flow through the tricuspid valve and absence of a color Doppler signal in the atretic aortic root. In addition, the left inferior pulmonary vein was identified. The left ventricular outflow tract view confirmed absence of color Doppler flow through the mitral valve, as well as an atretic aortic valve with absent flow. However, antegrade flow was seen through the tricuspid valve, and the left inferior pulmonary vein was also identified in this view. In the short-axis view of the great vessels/right ventricular outflow tract, the cross-section of the aorta was small when compared with the pulmonary artery. There was systolic perfusion across the pulmonary valve and trunk with aliasing at the ductus arteriosus. The ductal arch view demonstrated similar findings. The aortic arch view demonstrated a very narrow transverse aortic arch (coarctation), with reversed color Doppler flow in this area, as well as in the isthmus.

Interrupted inferior vena cava with azygos vein continuation and asplenia

In a 25-week fetus with asplenia and interrupted inferior vena cava with azygos vein continuation, six echocardiography views were abnormal using color Doppler FINE (Figure S1 and Videoclip S8). The karyotype following amniocentesis was 46XY and microarray results were normal. In the 3VT view, the azygos vein draining into the superior vena cava was visualized on both grayscale and color Doppler, with an opposite flow direction (red color) from that of the pulmonary artery and transverse aortic arch (blue color). In the four-chamber view, the 'double vessel' sign[74] was identified, with the cross-section of the descending aorta on the left side of the spine (red color) and the adjacent dilated azygos vein on the right side of the spine (absent Doppler signal). The four-chamber view was otherwise normal. Both the five-chamber and left ventricular outflow tract views were normal, except for the 'double vessel' sign. In the abdomen/stomach view, the stomach was located abnormally on the fetal right side. Moreover, VIS-Assistance was helpful in demonstrating the 'double

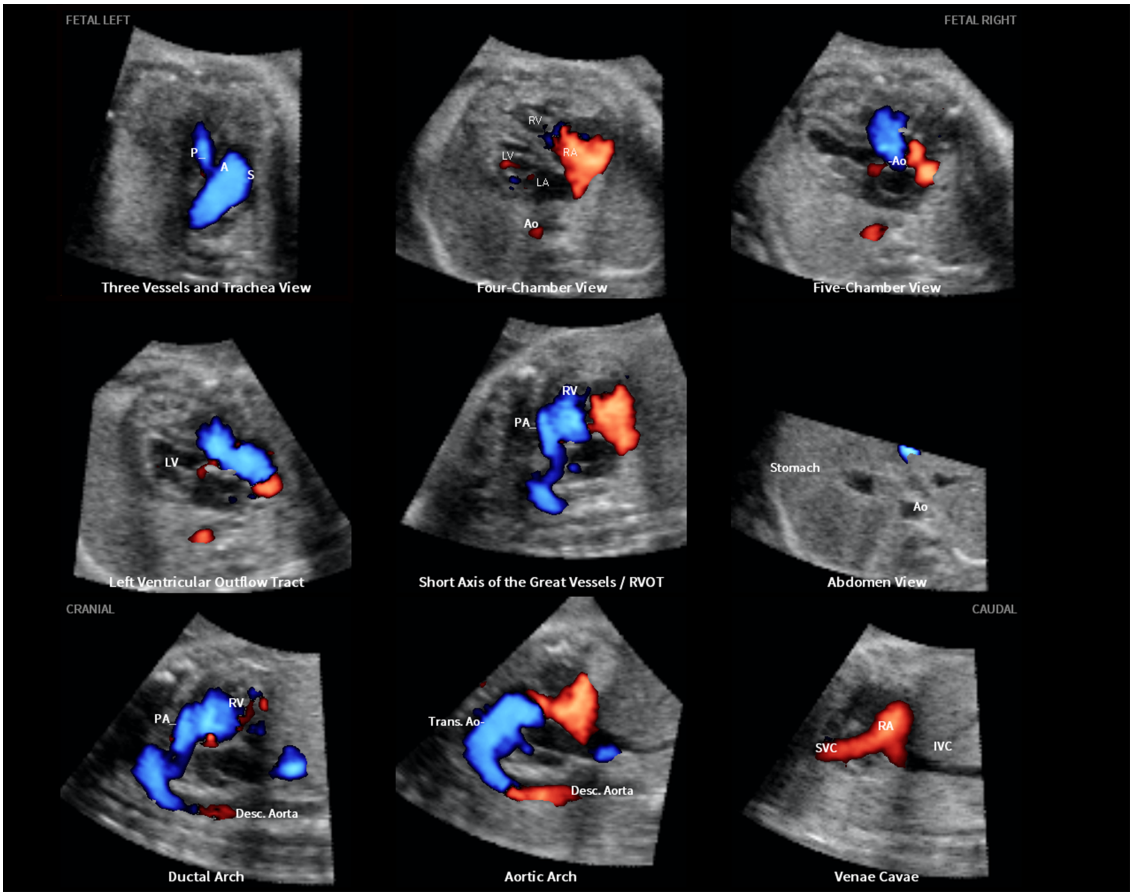

Figure 4 Application of color Doppler Fetal Intelligent Navigation Echocardiography method in 31-week fetus with tetralogy of Fallot (diagnostic planes with automatic labeling shown) (see Videoclip S6). Spatiotemporal image correlation volume acquired with S-flow Doppler ultrasound. Six echocardiography views were abnormal and demonstrate typical features of this cardiac defect. Three vessels and trachea view shows narrow pulmonary artery due to stenosis, while transverse aortic arch is prominent. There is 'Y-shaped' appearance of great vessels and antegrade flow (blue color) is seen. As is commonly noted in conotruncal abnormalities, four-chamber view appeared normal, with diastolic perfusion across both atrioventricular valves (see Videoclip S6). Both five-chamber and left ventricular outflow tract views show overriding aorta, dilated aortic root and perimembranous ventricular septal defect. Shunting of blood is seen from right ventricle across the ventricular septal defect into aortic root (five-chamber view) and large overriding aorta (left ventricular outflow tract view). In short-axis view of great vessels/right ventricular outflow tract, pulmonary artery is narrow with small ductus arteriosus and cross-section of aorta is dilated. Ductal arch demonstrates similar findings. S-flow Doppler signal was helpful in delineating anatomy of pulmonary artery and ductus arteriosus, as well as confirming antegrade flow in these structures. In aortic arch view, aortic root is dilated and there is prominent ascending aorta. A, transverse aortic arch; Ao, aorta; Desc., descending; IVC, inferior vena cava; LA, left atrium; LV, left ventricle; P, pulmonary artery; PA, pulmonary artery; RA, right atrium; RV, right ventricle; RVOT, right ventricular outflow tract; S, superior vena cava; SVC, superior vena cava; Trans., transverse.

vessel' sign, liver location (midline and left upper quadrant area of the abdomen), and cardiac apex pointing to the left side of the chest. Importantly, the superior and inferior venae cavae view demonstrated the prominent azygos vein arch (color Doppler flow in red) draining into the superior vena cava, as well as absence of the inferior vena cava. In addition, VIS-Assistance confirmed the stomach to be located on the right side of the abdomen and no inferior vena cava was visualized throughout the entire videoclip.

Coarctation of the aorta with tricuspid regurgitation (fetal hydrops)

A case was referred at 19 weeks of gestation for growth restriction, bilateral large cystic hygromas, bilateral pleural effusions and skin edema around the head, face, abdomen, lower extremities and dorsum of the feet. Amniocentesis revealed a karyotype consistent with Turner syndrome. STIC volume acquisition was performed in combination with S-flow Doppler ultrasound and five echocardiography views were abnormal using color Doppler FINE (Figure S2 and Videoclip S9). The 3VT showed narrowing of the transverse aortic arch compared with the main pulmonary artery; however, there was antegrade flow visualized. In the four-chamber view, there was ventricular disproportion, with the left side of the heart being smaller than the right; however, there was normal left ventricular filling in diastole. Due to increased color gain settings at the time of STIC volume acquisition, there was a bleeding artifact with superimposition of color over the atrioventricular valves, giving the false impression of a septal defect. Tricuspid regurgitation was evident during early to mid-systole and, as a result, the right atrium was dilated. Both the five-chamber and

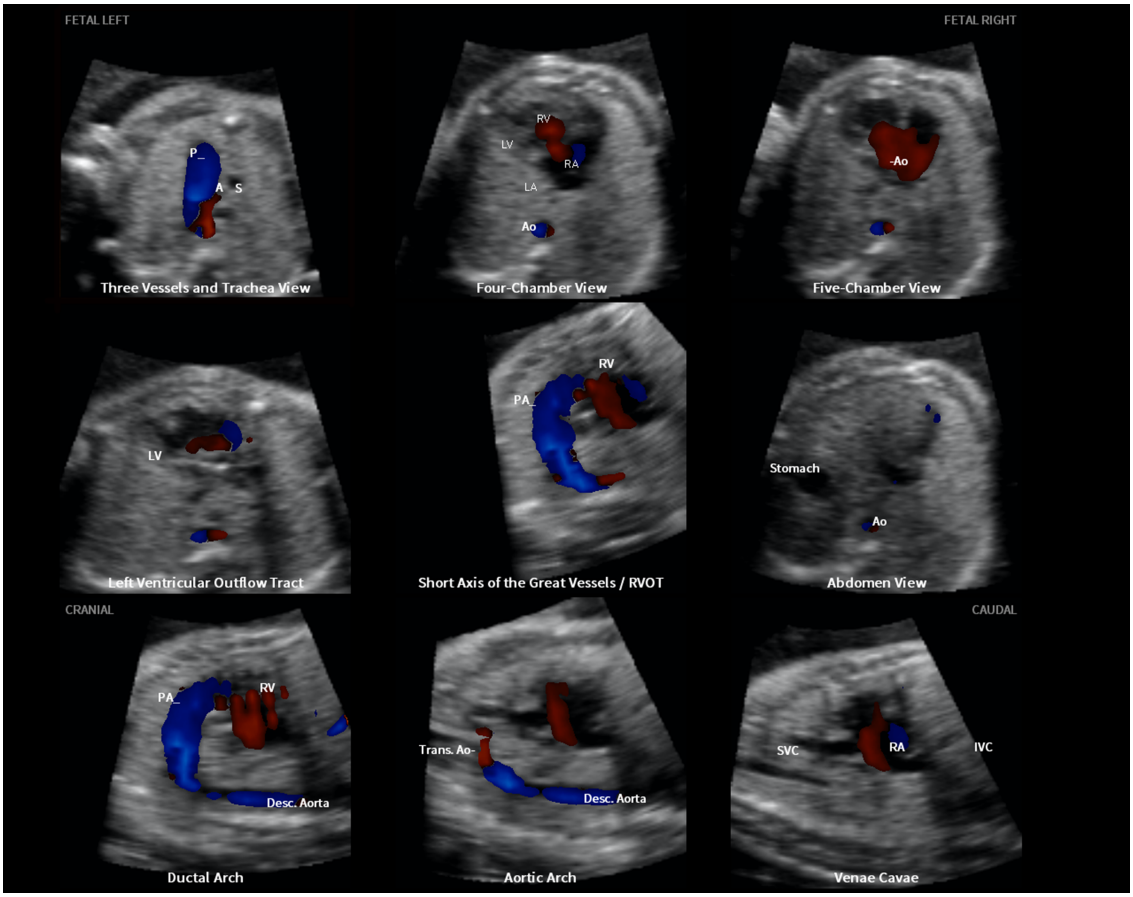

Figure 5 Application of color Doppler Fetal Intelligent Navigation Echocardiography method in 26-week fetus with hypoplastic left heart and coarctation of aorta (diagnostic planes with automatic labeling shown) (see Videoclip S7). Spatiotemporal image correlation volume was acquired with color Doppler ultrasound. Three vessels and trachea view shows hypoplastic transverse aortic arch with retrograde flow (red color), along with dilated pulmonary artery demonstrating antegrade flow (blue color). In four-chamber view, left side of heart is severely hypoplastic. There is antegrade flow through tricuspid valve during diastole, but absent flow through atretic mitral valve. Five-chamber view also demonstrates severely hypoplastic left side, antegrade flow through tricuspid valve and absence of color Doppler signal in atretic aortic root. Left ventricular outflow tract view confirms absence of color Doppler flow through mitral valve, as well as an atretic aortic valve with absent flow. However, antegrade flow is seen through the tricuspid valve. In short-axis view of great vessels/right ventricular outflow tract, cross-section of aorta is small when compared with pulmonary artery. There is systolic perfusion across pulmonary valve and trunk. Ductal arch view demonstrates similar findings. Aortic arch view demonstrates very narrow transverse aortic arch (coarctation), with reversed color Doppler flow in this area, as well as in the isthmus. A, transverse aortic arch; Ao, aorta; Desc., descending; IVC, inferior vena cava; LA, left atrium; LV, left ventricle; P, pulmonary artery; PA, pulmonary artery; RA, right atrium; RV, right ventricle; RVOT, right ventricular outflow tract; S, superior vena cava; SVC, superior vena cava; Trans., transverse.

left ventricular outflow tract views showed a narrow aortic root and aorta, respectively; however, there was antegrade flow across the aortic valve. Coarctation of the aorta was demonstrated in the aortic arch view, with narrowing of the transverse aortic arch. However, there was no reversal of the S-flow Doppler signal or color aliasing.

Taken together, color Doppler FINE was able to demonstrate abnormal cardiac anatomy (via grayscale information alone) and provided additional diagnostic information in all four cases of CHD.

Other clinical applications of color Doppler FINE

During the analysis of STIC volumes of normal fetal hearts by color Doppler FINE technology, we noted various applications that may be useful in the clinical setting.

(1) Depicting cardiac structures successfully when grayscale does not: color Doppler ultrasound facilitates recognition of fetal cardiac anatomy when 2D imaging is suboptimal[20,21]. Similarly, color Doppler FINE allowed depiction of cardiac structures even though this was not apparent or was unclear on grayscale. Both color and S-flow Doppler combined with STIC technology were particularly helpful in visualizing the ductus arteriosus/ductal arch, as well as the aortic arch. For example, although the grayscale image was not able to truly depict the ductus arteriosus, color Doppler FINE was able to demonstrate such structure and the ductal arch easily.

(2) Tricuspid regurgitation: an important question is whether depiction of color/S-flow Doppler in the STIC volume dataset modified the initial diagnostic impression gained by grayscale only. Of the 37 fetuses

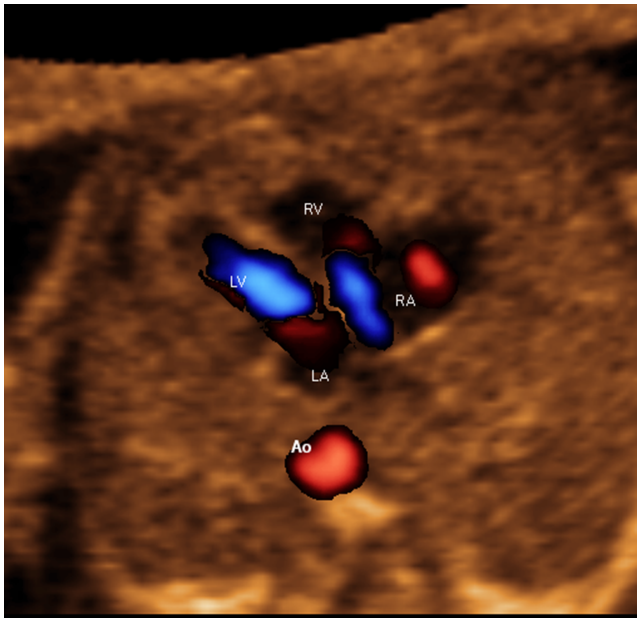

Figure 6 Trivial tricuspid regurgitation in early systole demonstrated through color Doppler Fetal Intelligent Navigation Echocardiography in normal fetus (see Videoclip S10). Spatiotemporal image correlation volume was acquired with S-flow Doppler ultrasound. Four-chamber view diagnostic plane in grayscale was completely normal. However, S-flow Doppler depicted tricuspid regurgitation. Automatic labeling (through intelligent navigation) of chambers in four-chamber view and descending aorta (Ao) is shown. LA, left atrium; LV, left ventricle; RA, right atrium; RV, right ventricle.

Figure 7 Spatiotemporal image correlation volume dataset of normal fetal heart acquired with S-flow Doppler imaging and analyzed by color Doppler Fetal Intelligent Navigation Echocardiography (four-chamber view with automatic labeling shown). Right inferior pulmonary vein can be visualized along imaginary straight line coursing backwards from atrial septum. Vein is seen with color flow towards left atrium (red color), at site of atrial septum (see Videoclip S11). Ao, aorta; LA, left atrium; LV, left ventricle; RA, right atrium; RV, right ventricle.

with normal hearts, 8% ($n = 3$) showed a completely normal four-chamber view diagnostic plane in grayscale. However, S-flow Doppler depicted trivial tricuspid regurgitation in early systole (Figure 6, Videoclip S10). None of the three neonates had cardiac issues after birth.

(3) Venous system (systemic and pulmonary): to demonstrate the fetal venous system (e.g. pulmonary and caval veins), low-scale color Doppler presets are required in most cases[13]. Color Doppler FINE was able to depict several fetal venous structures in the 3VT, four-chamber, five-chamber, stomach/abdomen and vena cava views. These included the hepatic veins, ductus venosus, superior and inferior venae cavae and azygos vein. The inferior vena cava is widened as it enters the right atrium due to the confluence of the ductus venosus and hepatic veins[13] and this was also demonstrated via color Doppler FINE in the superior and inferior venae cavae view. Yet, the fetal venous system overall was not necessarily depicted via color or S-flow Doppler in all STIC volumes since a high velocity scale had been used. However, we found that lowering the color threshold in post-processing was helpful in depicting venous structures.

Regarding the fetal pulmonary veins, it is generally difficult to image all four veins even when using color Doppler ultrasound; however, the right and left inferior veins can be imaged[13,27]. The right inferior pulmonary vein can be visualized along an imaginary straight line coursing backwards from the atrial septum[27]. Using color Doppler FINE, such a vein could be seen with color flow towards the left atrium (red color), at the site of the atrial septum (Figure 7 and Videoclip S11). However, this was seen only occasionally, because the velocity range was not low enough (e.g. 15–25 cm/s)[6,27]. On the other hand, the left inferior pulmonary vein appears as a vessel pointing directly towards the foramen ovale flap on color Doppler imaging (i.e. closer to 90°)[27]. Due to the insonation angle of such a vein, it was even less frequently identified (*vs* right inferior pulmonary vein) in the study herein. Using color Doppler FINE, we did not formally evaluate the frequency of depicting the pulmonary veins via color or S-flow Doppler for the current study, as this would have required low velocity settings at the time of STIC volume acquisition[13], as well as acquisitions in which the pulmonary veins are more parallel to the angle of insonation. However, as described above, we recorded how often the pulmonary veins could be demonstrated on grayscale in the four-chamber view diagnostic plane and VIS-Assistance.

(4) Foramen ovale flow (interatrial flow): using color Doppler FINE, flow via color or S-flow Doppler across the foramen ovale was identified for the following views (using diagnostic plane/VIS-Assistance): (a) four chamber: 19% (5/27) and 33% (11/33) of cases, respectively; and (b) short-axis view of the great vessels/right ventricular outflow tract: 19% (5/27) and 36% (12/33) of cases, respectively. Foramen ovale flow was not more frequently identified because STIC volumes had been acquired from an apical four-chamber view with the spine located posteriorly. Therefore, foramen ovale flow was almost perpendicular to the transducer beam during the actual

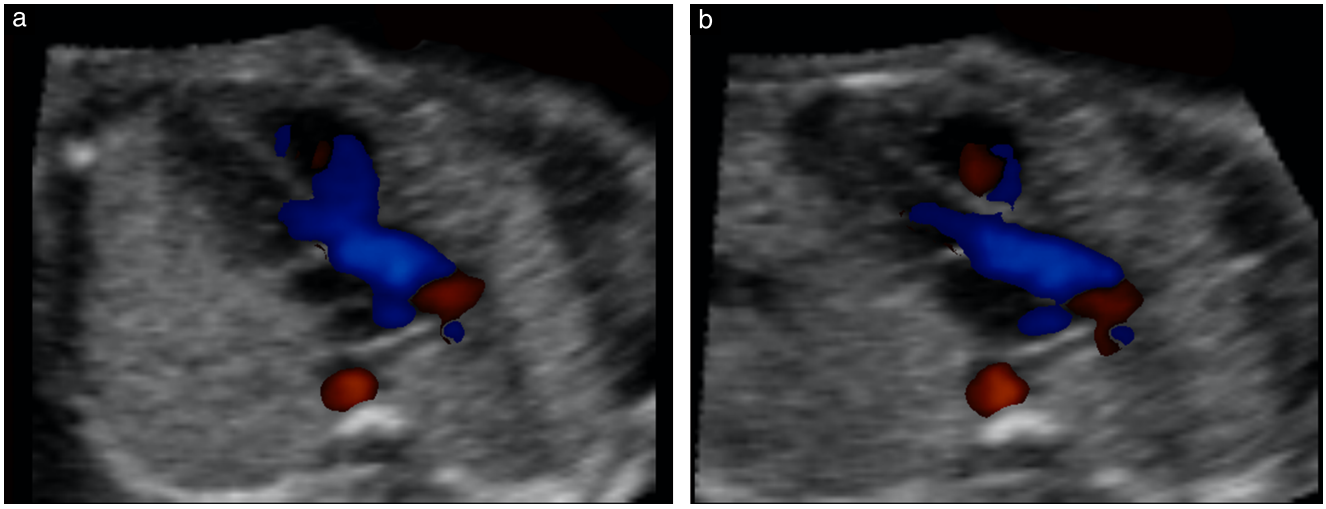

Figure 8 'Pseudo' ventricular septal defect (VSD) in left ventricular outflow tract view, as depicted by color Doppler. This spatiotemporal image correlation volume dataset of normal fetal heart was acquired with color Doppler imaging and analyzed by color Doppler Fetal Intelligent Navigation Echocardiography. (a) Diagnostic plane shows color signal (blue) from right ventricle crossing over anterior wall of aorta and spilling into left ventricular outflow tract, giving 'Y' appearance. (b) After Virtual Intelligent Sonographer Assistance was activated, automatic navigational movements improved echocardiography view and pseudo-VSD was no longer visualized. No settings (e.g. color threshold, balance) were changed between (a) and (b).

acquisition. To depict color Doppler flow across the foramen ovale, a lateral four-chamber view is required for the STIC volume acquisition to allow angle-appropriate alignment of the Doppler cursor with flow direction[4].

General applications of color Doppler FINE: various scenarios

There are several points about the general application of color Doppler FINE that are worth noting and are detailed in Table S1. They include various scenarios and suggested recommendations to resolve them: (1) the relationship between the depiction of fetal cardiac structures and the angle of insonation of the ultrasound beam; (2) how a 'pseudo' ventricular septal defect can occur (Figure 8); (3) cardiac structures not demonstrating a color/S-flow Doppler signal; (4) cardiac structures that demonstrate the opposite color/S-flow Doppler signal from what is expected; and (5) too much color/S-flow Doppler signal.

It is noteworthy that once a STIC volume has been acquired in combination with color or S-flow Doppler, the only color parameters that may be adjusted in post-processing are the threshold and balance. The velocity scale (or PRF) and gain settings have already been incorporated into the volume dataset. Therefore, using color Doppler FINE, the venae cavae or pulmonary veins may not be seen as frequently as when compared with live 2D sonography, when both color gain and the velocity scale can be adjusted in real time.

The success rates of generating the superior and inferior venae cavae view with appropriate color and S-flow Doppler information using color Doppler FINE was only 33% (Table 3) and 30% (Table 4), respectively. In addition, there was absent color or S-flow Doppler information in the superior vena cava of the 3VT view in 74% and 67% of cases, respectively (Tables 3 and 4). Such results can be explained because (1) during STIC volume acquisition of the apical four-chamber view, the direction of caval blood flow was perpendicular to the angle of insonation of the ultrasound beam, and therefore there was attenuation of the Doppler frequency shift, with a resulting decrease in the color signal; and (2) Doppler settings were intentionally set to a high velocity flow to interrogate the atrioventricular valves and great vessels, which led to reduced color sensitivity in the venae cavae. Assessment of caval veins using color Doppler ultrasound requires lower velocity scales (e.g. 10–20 cm/s)[28]. For the study population herein, S-flow Doppler did not improve the success rate of depicting a color signal in the superior and inferior venae cavae view and is most likely due to the presets for this modality that were implemented.

Nevertheless, STIC volume datasets acquired with S-flow Doppler and analyzed by color Doppler FINE allowed (1) depiction of pulmonary veins (four- and five-chamber views), and (2) persistence of the same Doppler signal (e.g. blue color) throughout the cardiac cycle. Further study is required to delineate the advantages, if any, of S-flow Doppler (*vs* color Doppler) STIC volume datasets analyzed by FINE.

DISCUSSION

Principal findings of the study

After applying the FINE method to STIC volume datasets acquired with color or S-flow Doppler ultrasound in the second and third trimesters (1) nine fetal echocardiography views in grayscale (color or S-flow Doppler information turned off) were generated successfully using diagnostic planes in 73–100% of cases, VIS-Assistance

in 100% of cases and a combination of diagnostic planes and/or VIS-Assistance in 100% of cases; (2) eight fetal echocardiography views with appropriate color and S-flow Doppler information were generated successfully in 89–100% and 91–100% of cases, respectively, using a combination of diagnostic planes and/or VIS-Assistance; however, the success rate for the ninth fetal echocardiography view (i.e. superior and inferior venae cavae) was 33% and 30% of cases for color and S-flow Doppler, respectively; and (3) in cases of CHD, color Doppler FINE demonstrated successfully abnormal fetal cardiac anatomy and/or hemodynamic flow. Taken together, these findings suggest that color Doppler FINE is a reliable and informative method to examine the normal and abnormal fetal heart.

Color Doppler combined with STIC technology

While the use of color Doppler ultrasound is not considered mandatory in sonographic screening of the fetal heart, becoming familiar with this modality and adding this to routine screening has recently been encouraged[5]. This study demonstrates, for the first time, the clinical feasibility of applying FINE technology to STIC volumes of normal and abnormal fetal hearts acquired with either color or bidirectional power Doppler information. In a previous study, STIC volume datasets were acquired with color Doppler sonography and analyzed using tomographic ultrasound imaging (TUI)[75]. The four-chamber, five-chamber and 3VT views were visualized in 98.2%, 97.0% and 83.6% of such volumes, respectively. However, through color Doppler FINE, we noted an improved performance. The four-chamber, five-chamber and 3VT views with appropriate Doppler information were obtained successfully in 100%, 89% and 100% of cases by color Doppler and 91%, 100% and 100% of cases by S-flow Doppler (Tables 3 and 4). The success rate of obtaining the five-chamber view with appropriate color Doppler information was not 100% because in these three cases (Table 3), there was no color flow in the aortic root, which can be attributed to a perpendicular angle of insonation in the STIC volume acquisitions. Therefore, this is not a true 'failure' of color Doppler FINE. Similarly, the success rate of obtaining the four-chamber view with appropriate S-flow Doppler information through color Doppler FINE was only 91% (30/33) (Table 4), because, in these three cases, trivial tricuspid regurgitation in early systole was identified. Otherwise, the four-chamber views were obtained successfully.

In a second study of fetuses between 18 and 35 weeks of gestation, Chaoui *et al.* demonstrated successfully the four-chamber, five-chamber and 3VT views using manual navigation in 89% (31/35) of healthy fetuses and 89% (24/27) of fetuses with CHD[30]. Yet, through color Doppler FINE, for each color or S-flow Doppler STIC volume dataset of normal hearts, 93% and 94% of volumes demonstrated either eight or all nine echocardiography views, respectively. Moreover, for the CHD cases herein, nine fetal echocardiography views were generated successfully by color Doppler FINE with either color or S-flow Doppler information depicted.

Benefits of color Doppler FINE

The current study is different from others[30,75] in that neither manual navigation[70] nor TUI was used to generate fetal echocardiography views from STIC volume datasets. Instead, intelligent navigation technology was implemented[70]. As a result, there was reduced operator dependency and examination of the fetal heart was standardized and simplified[62]. Moreover, the FINE method uniquely allows automatic labeling of anatomical structures and echocardiography views[62,70].

Other benefits of color Doppler FINE technology include the following. (1) Nine echocardiography views are generated simultaneously with Doppler flow information in a single template, including both transverse and longitudinal planes (Figures 1 and 2, Videoclips S2 and S3). This is in contrast to manual navigation through a STIC volume dataset[70] or real-time 2D sonography, in which cardiac views are obtained sequentially[7]. Moreover, TUI cannot depict both transverse and longitudinal planes at the same time. Therefore, since nine echocardiography views with Doppler flow are demonstrated simultaneously, the same information may be viewed in several planes. For example, systolic Doppler flow through the great vessels is demonstrated in the 3VT, five-chamber, left ventricular outflow tract, short-axis view of great vessels/right ventricular outflow tract, ductal arch, and aortic arch views. We found this feature particularly helpful in cases of CHD, as well as for education and teaching purposes. (2) It modifies the initial diagnostic impression obtained through grayscale in the STIC volume dataset for both normal fetuses (e.g. depicts trivial physiological tricuspid regurgitation) and those with CHD. (3) Removal of color and power Doppler information allows successful examination of the fetal heart through grayscale. Although we were initially concerned that implementing color and S-flow Doppler sonography as well as a large color 'region of interest' box over the fetal heart would decrease the frame rate sufficiently to degrade the quality of STIC volumes, this was not the case. The implication is that additional STIC volumes in grayscale do not necessarily need to be acquired to generate echocardiography views. (4) It allows depiction of cardiac structures that were not apparent on grayscale. (5) For CHD cases, it corroborates the anatomical diagnosis and defines both normal and abnormal hemodynamic flow. (6) It mimics real-time color Doppler examination of the fetal heart due to its motion characteristics. (7) Color VIS-Assistance technology: (a) by improving the success of generating a given cardiac view, an appropriate Doppler signal becomes visible (Table S1); (b) allows visualization of more anatomical structures (e.g. hepatic veins); and (c) reduces false-positive diagnoses, such as a 'pseudo' ventricular septal defect (Table S1).

It should be noted that the application of color Doppler FINE is not meant to replace real-time fetal echocardiography, which can evaluate cardiac rate and rhythm disturbances, and allows the performance of pulsed Doppler velocimetry and cardiac biometry.

Conclusions

The FINE method applied to STIC volume datasets acquired with color and bidirectional power Doppler provides clinically useful information about cardiac structure and function in fetuses with normal hearts. For cases of congenital heart disease, abnormal fetal cardiac anatomy and hemodynamic flow characteristics can be depicted. These findings suggest that there is diagnostic potential for color Doppler FINE in the evaluation of fetuses with normal hearts, as well as in cases of congenital heart disease. Future studies are required to validate the diagnostic utility of this new technology.

ACKNOWLEDGMENTS

This work was made possible by a partnership with two unique and outstanding computer scientists, Mr Gustavo Abella and Mr Ricardo Gayoso. An application for a patent ('Apparatus and Method for Fetal Intelligent Navigation Echocardiography') has been filed with the US Patent and Trademark Office and the patent is pending. L.Y. and R.R. are co-inventors, along with Mr Abella and Mr Gayoso. The rights of L.Y. and R.R. have been assigned to Wayne State University and NICHD/NIH, respectively. None of the authors has a financial relationship with either Samsung Healthcare, Seoul, Korea or Medge Platforms, Inc., New York, NY, USA.

The work of R.R. was supported by the Perinatology Research Branch, Division of Intramural Research, *Eunice Kennedy Shriver* National Institute of Child Health and Human Development, NIH, DHHS. R.R. has contributed to this work as part of his official duties as an employee of the United States Federal Government. L.Y. was funded by Wayne State University through a service contract in support of the Perinatology Research Branch. The contributions of Mr Abella and Mr Gayoso were funded by Medge Platforms, Inc., New York, NY, USA.

This research was supported, in part, by the Perinatology Research Branch, Division of Intramural Research, *Eunice Kennedy Shriver* National Institute of Child Health and Human Development, National Institutes of Health, Department of Health and Human Services (NICHD/NIH); and, in part, with Federal funds from NICHD, NIH under Contract No. HHSN275201300006C.

REFERENCES

1. Kremkau FK. Principles of color flow imaging. *J Vasc Tech* 1991; **15**: 104–109.
2. Omoto R, Kasai C. Physics and instrumentation of Doppler color flow mapping. *Echocardiography* 1987; **4**: 467–483.
3. Lee R. Physical principles of flow mapping in cardiology. In *Textbook of Color Doppler Echocardiography*, Nanda NC (ed). Lea & Febiger: Philadelphia, 1989; **18**.
4. Maulik D. Sonographic color flow mapping: basic principles. In *Doppler Ultrasound in Obstetrics and Gynecology*, Maulik D (ed). Springer-Verlag: Berlin, Heidelberg, 2005; 69–84.
5. Carvalho JS, Allan LD, Chaoui R, Copel JA, DeVore GR, Hecher K, Lee W, Munoz H, Paladini D, Tutschek B, Yagel S. ISUOG practice guidelines (updated): sonographic screening examination of the fetal heart. *Ultrasound Obstet Gynecol* 2013; **41**: 348–359.
6. Chaoui R, McEwing R. Three cross-sectional planes for fetal color Doppler echocardiography. *Ultrasound Obstet Gynecol* 2003; **21**: 81–93.
7. Donofrio MT, Moon-Grady AJ, Hornberger LK, Copel JA, Sklansky MS, Abuhamad A, Cuneo BF, Huhta JC, Jonas RA, Krishnan A, Lacey S, Lee W, Michelfelder EC Sr, Rempel GR, Silverman NH, Spray TL, Strasburger JF, Tworetzky W, Rychik J; American Heart Association Adults With Congenital Heart Disease Joint Committee of the Council on Cardiovascular Disease in the Young and Council on Clinical Cardiology, Council on Cardiovascular Surgery and Anesthesia, and Council on Cardiovascular and Stroke Nursing. Diagnosis and treatment of fetal cardiac disease: a scientific statement from the American Heart Association. *Circulation* 2014; **129**: 2183–2242.
8. Lee W, Allan L, Carvalho JS, Chaoui R, Copel J, Devore G, Hecher K, Munoz H, Nelson T, Paladini D, Yagel S; ISUOG Fetal Echocardiography Task Force. ISUOG consensus statement: what constitutes a fetal echocardiogram? *Ultrasound Obstet Gynecol* 2008; **32**: 239–242.
9. DeVore GR. Color Doppler examination of the outflow tracts of the fetal heart: a technique for identification of cardiovascular malformations. *Ultrasound Obstet Gynecol* 1994; **4**: 463–471.
10. Zhang Y, Ding C, Fan M, Ren W, Guo Y, Sun W, Cai A. Evaluation of normal fetal pulmonary veins using B-flow imaging with spatiotemporal image correlation and by traditional color Doppler echocardiography. *Prenat Diagn* 2012; **32**: 1186–1191.
11. Lei W, Ying Z, Ailu C, Xiaoguang W. Evaluation of normal fetal ductus venosus using B-flow imaging with spatiotemporal image correlation and traditional color Doppler echocardiography. *Echocardiography* 2015; **32**: 325–331.
12. Benacerraf BR, Sanders SP. Fetal echocardiography. *Radiol Clin North Am* 1990; **28**: 131–147.
13. Sinkovskaya E, Klassen A, Abuhamad A. A novel systematic approach to the evaluation of the fetal venous system. *Semin Fetal Neonatal Med* 2013; **18**: 269–278.
14. Maulik D, Nanda NC, Hsiung MC, Youngblood JP. Doppler color flow mapping of the fetal heart. *Angiology* 1986; **37**: 628–632.
15. Copel JA, Hobbins JC, Kleinman CS. Doppler echocardiography and color flow mapping. *Obstet Gynecol Clin North Am* 1991; **18**: 845–851.
16. Chiba Y, Kanzaki T, Kobayashi H, Murakami M, Yutani C. Evaluation of fetal structural heart disease using color flow mapping. *Ultrasound Med Biol* 1990; **16**: 221–229.
17. Copel JA, Morotti R, Hobbins JC, Kleinman CS. The antenatal diagnosis of congenital heart disease using fetal echocardiography: is color flow mapping necessary? *Obstet Gynecol* 1991; **78**: 1–8.
18. Abuhamad A. Color and pulsed Doppler in fetal echocardiography. *Ultrasound Obstet Gynecol* 2004; **24**: 1–9.
19. Chaoui R, Heling KS. New developments in fetal heart scanning: three- and four-dimensional fetal echocardiography. *Semin Fetal Neonatal Med* 2005; **10**: 567–577.
20. Stewart PA, Wladimiroff JW. Fetal echocardiography and color Doppler flow imaging: the Rotterdam experience. *Ultrasound Obstet Gynecol* 1993; **3**: 168–175.
21. Gardiner H, Chaoui R. The fetal three-vessel and tracheal view revisited. *Semin Fetal Neonatal Med* 2013; **18**: 261–268.
22. DeVore GR, Horenstein J, Siassi B, Platt LD. Fetal echocardiography. VII. Doppler color flow mapping: a new technique for the diagnosis of congenital heart disease. *Am J Obstet Gynecol* 1987; **156**: 1054–1064.
23. Sharland GK, Chita SK, Allan LD. The use of colour Doppler in fetal echocardiography. *Int J Cardiol* 1990; **28**: 229–236.
24. Gembruch U, Chatterjee MS, Bald R, Redel DA, Hansmann M. Color Doppler flow mapping of fetal heart. *J Perinat Med* 1991; **19**: 27–32.
25. Nadel AS. Addition of color Doppler to the routine obstetric sonographic survey aids in the detection of pulmonic stenosis. *Fetal Diagn Ther* 2010; **28**: 175–179.
26. Del Bianco A, Russo S, Lacerenza N, Rinaldi M, Rinaldi G, Nappi L, Greco P. Four chamber view plus three-vessel and trachea view for a complete evaluation of the fetal heart during the second trimester. *J Perinat Med* 2006; **34**: 309–312.
27. Chaoui R, Kalache KD. Three-dimensional color and power Doppler ultrasonography of the fetal cardiovascular system. In *Doppler Ultrasound in Obstetrics and Gynecology*, Maulik D (ed). Springer-Verlag: Berlin, Heidelberg, 2005; 85–94.
28. Abuhamad A, Chaoui R. Color Doppler in fetal echocardiography. In *A Practical Guide to Fetal Echocardiography: Normal and Abnormal Hearts*, Abuhamad A, Chaoui R (eds). Wolters Kluwer: Philadelphia, 2016; 144–159.
29. Heling KS, Chaoui R, Bollmann R. Advanced dynamic flow – a new method of vascular imaging in prenatal medicine. A pilot study of its applicability. *Ultraschall Med* 2004; **25**: 280–284.
30. Chaoui R, Hoffmann J, Heling KS. Three-dimensional (3D) and 4D color Doppler fetal echocardiography using spatio-temporal image correlation (STIC). *Ultrasound Obstet Gynecol* 2004; **23**: 535–545.
31. AboEllail MA, Kanenishi K, Tenkumo C, Kawanishi K, Kaji T, Hata T. Diagnosis of truncus arteriosus in first trimester of pregnancy using transvaginal four-dimensional color Doppler ultrasound. *Ultrasound Obstet Gynecol* 2015; **45**: 759–760.
32. Bennasar M, Martínez JM, Olivella A, del Río M, Gómez O, Figueras F, Puerto B, Gratacós E. Feasibility and accuracy of fetal echocardiography using four-dimensional spatiotemporal image correlation technology before 16 weeks' gestation. *Ultrasound Obstet Gynecol* 2009; **33**: 645–651.
33. Gonçalves LF, Romero R, Espinoza J, Lee W, Treadwell M, Chintala K, Brandl H, Chaiworapongsa T. Four-dimensional ultrasonography of the fetal heart using color Doppler spatiotemporal image correlation. *J Ultrasound Med* 2004; **23**: 473–481.

34. Gonçalves LF, Lee W, Espinoza J, Romero R. Examination of the fetal heart by four-dimensional (4D) ultrasound with spatio-temporal image correlation (STIC). *Ultrasound Obstet Gynecol* 2006; **27**: 336–348.
35. Bennasar M, Martínez JM, Gómez O, Figueras F, Olivella A, Puerto B, Gratacós E. Intra- and interobserver repeatability of fetal cardiac examination using four-dimensional spatiotemporal image correlation in each trimester of pregnancy. *Ultrasound Obstet Gynecol* 2010; **35**: 318–323.
36. Yagel S, Valsky DV, Messing B. Detailed assessment of fetal ventricular septal defect with 4D color Doppler ultrasound using spatio-temporal image correlation technology. *Ultrasound Obstet Gynecol* 2005; **25**: 97–98.
37. Turan S, Turan OM, Desai A, Harman CR, Baschat AA. First-trimester fetal cardiac examination using spatiotemporal image correlation, tomographic ultrasound and color Doppler imaging for the diagnosis of complex congenital heart disease in high-risk patients. *Ultrasound Obstet Gynecol* 2014; **44**: 562–567.
38. Bennasar M, Martínez JM, Gómez O, Bartrons J, Olivella A, Puerto B, Gratacós E. Accuracy of four-dimensional spatiotemporal image correlation echocardiography in the prenatal diagnosis of congenital heart defects. *Ultrasound Obstet Gynecol* 2010; **36**: 458–464.
39. Espinoza J, Lee W, Comstock C, Romero R, Yeo L, Rizzo G, Paladini D, Viñals F, Achiron R, Gindes L, Abuhamad A, Sinkovskaya E, Russell E, Yagel S. Collaborative study on 4-dimensional echocardiography for the diagnosis of fetal heart defects: the COFEHD study. *J Ultrasound Med* 2010; **29**: 1573–1580.
40. Devore GR, Sklansky MS. Three-dimensional imaging of the fetal heart: current applications and future directions. *Prog Pediatr Cardiol* 2006; **22**: 9–29.
41. Espinoza J. Contemporary clinical applications of spatio-temporal image correlation in prenatal diagnosis. *Curr Opin Obstet Gynecol* 2011; **23**: 94–102.
42. Ghi T, Cera E, Segata M, Michelacci L, Pilu G, Pelusi G. Inversion mode spatio-temporal image correlation (STIC) echocardiography in three-dimensional rendering of fetal ventricular septal defects. *Ultrasound Obstet Gynecol* 2005; **26**: 679–680.
43. Gindes L, Hegesh J, Weisz B, Gilboa Y, Achiron R. Three and four dimensional ultrasound: a novel method for evaluating fetal cardiac anomalies. *Prenat Diagn* 2009; **29**: 645–653.
44. Hata T, Kanenishi K, Mori N, Yazon AO, Hanaoka U, Tanaka H. Four-dimensional color Doppler reconstruction of the fetal heart with glass-body rendering mode. *Am J Cardiol* 2014; **114**: 1603–1606.
45. He Y, Wang J, Gu X, Zhang Y, Han J, Liu X, Li Z. Application of spatio-temporal image correlation technology in the diagnosis of fetal cardiac abnormalities. *Exp Ther Med* 2013; **5**: 1637–1642.
46. Ionescu C. The benefits of 3D-4D fetal echocardiography. *Maedica (Buchar)* 2010; **5**: 45–50.
47. Lima AI, Araujo Júnior E, Martins WP, Nardozza LM, Moron AF, Pares DB. Assessment of the fetal heart at 12–14 weeks of pregnancy using B-mode, color Doppler, and spatiotemporal image correlation via abdominal and vaginal ultrasonography. *Pediatr Cardiol* 2013; **34**: 1577–1582.
48. Viñals F, Ascenzo R, Naveas R, Huggon I, Giuliano A. Fetal echocardiography at 11 + 0 to 13 + 6 weeks using four-dimensional spatiotemporal image correlation telemedicine via an Internet link: a pilot study. *Ultrasound Obstet Gynecol* 2008; **31**: 633–638.
49. Messing B, Porat S, Imbar T, Valsky DV, Anteby EY, Yagel S. Mild tricuspid regurgitation: a benign fetal finding at various stages of pregnancy. *Ultrasound Obstet Gynecol* 2005; **26**: 606–609.
50. Tudorache S, Cara M, Iliescu DG, Novac L, Cernea N. First trimester two- and four-dimensional cardiac scan: intra- and interobserver agreement, comparison between methods and benefits of color Doppler technique. *Ultrasound Obstet Gynecol* 2013; **42**: 659–668.
51. Turan S, Turan O, Baschat AA. Three- and four-dimensional fetal echocardiography. *Fetal Diagn Ther* 2009; **25**: 361–372.
52. Votino C, Cos T, Abu-Rustum R, Dahman Saidi S, Gallo V, Dobrescu O, Dessy H, Jani J. Use of spatiotemporal image correlation at 11–14 weeks' gestation. *Ultrasound Obstet Gynecol* 2013; **42**: 669–678.
53. Yagel S, Cohen SM, Rosenak D, Messing B, Lipschuetz M, Shen O, Valsky DV. Added value of three-/four-dimensional ultrasound in offline analysis and diagnosis of congenital heart disease. *Ultrasound Obstet Gynecol* 2011; **37**: 432–437.
54. Paladini D, Volpe P, Sglavo G, Vassallo M, De Robertis V, Marasini M, Russo MG. Transposition of the great arteries in the fetus: assessment of the spatial relationships of the arterial trunks by four-dimensional echocardiography. *Ultrasound Obstet Gynecol* 2008; **31**: 271–276.
55. Paladini D, Vassallo M, Sglavo G, Lapadula C, Martinelli P. The role of spatio-temporal image correlation (STIC) with tomographic ultrasound imaging (TUI) in the sequential analysis of fetal congenital heart disease. *Ultrasound Obstet Gynecol* 2006; **27**: 555–561.
56. Turan S, Turan OM, Maisel P, Gaskin P, Harman CR, Baschat AA. Three dimensional sonography in the prenatal diagnosis of aortic arch abnormalities. *J Clin Ultrasound* 2009; **37**: 253–257.
57. Adriaanse BM, van Vugt JM, Haak MC. Three- and four-dimensional ultrasound in fetal echocardiography: an up-to-date overview. *J Perinatol* 2016; **36**: 685–693.
58. Turan S, Turan OM, Ty-Torredes K, Harman CR, Baschat AA. Standardization of the first-trimester fetal cardiac examination using spatiotemporal image correlation with tomographic ultrasound and color Doppler imaging. *Ultrasound Obstet Gynecol* 2009; **33**: 652–656.
59. Gonçalves LF, Espinoza J, Romero R, Lee W, Beyer B, Treadwell MC, Humes R. A systematic approach to prenatal diagnosis of transposition of the great arteries using 4-dimensional ultrasonography with spatiotemporal image correlation. *J Ultrasound Med* 2004; **23**: 1225–1231.
60. Tonni G, Centini G, Taddei F. Can 3D ultrasound and Doppler angiography of great arteries be included in second trimester echocardiographic examination? A prospective study on low-risk pregnancy population. *Echocardiography* 2009; **26**: 815–822.
61. Avnet H, Mazaaki E, Shen O, Cohen S, Yagel S. Evaluating spatiotemporal image correlation technology as a tool for training nonexpert sonographers to perform examinations of the fetal heart. *J Ultrasound Med* 2016; **35**: 111–119.
62. Yeo L, Romero R. Fetal Intelligent Navigation Echocardiography (FINE): a novel method for rapid, simple, and automatic examination of the fetal heart. *Ultrasound Obstet Gynecol* 2013; **42**: 268–284.
63. Garcia M, Yeo L, Romero R, Haggerty D, Giardina I, Hassan SS, Chaiworapongsa T, Hernandez-Andrade E. Prospective evaluation of the fetal heart using Fetal Intelligent Navigation Echocardiography (FINE). *Ultrasound Obstet Gynecol* 2016; **47**: 450–459.
64. Veronese P, Bogana G, Cerutti A, Yeo L, Romero R, Gervasi MT. A prospective study of the use of Fetal Intelligent Navigation Echocardiography (FINE) to obtain standard fetal echocardiography views. *Fetal Diagn Ther* 2017; **41**: 89–99.
65. Yeo L, Romero R. How to acquire cardiac volumes for sonographic examination of the fetal heart: Part 1. *J Ultrasound Med* 2016; **35**: 1021–1042.
66. Viñals F, Poblete P, Giuliano A. Spatio-temporal image correlation (STIC): a new tool for the prenatal screening of congenital heart defects. *Ultrasound Obstet Gynecol* 2003; **22**: 388–394.
67. DeVore GR, Falkensammer P, Sklansky MS, Platt LD. Spatio-temporal image correlation (STIC): new technology for evaluation of the fetal heart. *Ultrasound Obstet Gynecol* 2003; **22**: 380–387.
68. Yeo L, Romero R. How to acquire cardiac volumes for sonographic examination of the fetal heart: Part 2. *J Ultrasound Med* 2016; **35**: 1043–1066.
69. Gonçalves LF, Lee W, Chaiworapongsa T, Espinoza J, Schoen ML, Falkensammer P, Treadwell M, Romero R. Four-dimensional ultrasonography of the fetal heart with spatiotemporal image correlation. *Am J Obstet Gynecol* 2003; **189**: 1792–1802.
70. Yeo L, Romero R. Intelligent navigation to improve obstetrical sonography. *Ultrasound Obstet Gynecol* 2016; **47**: 403–409.
71. Bhide A, Acharya G, Bilardo CM, Brezinka C, Cafici D, Hernandez-Andrade E, Kalache K, Kingdom J, Kiserud T, Lee W, Lees C, Leung KY, Malinger G, Mari G, Prefumo F, Sepulveda W, Trudinger B. ISUOG practice guidelines: use of Doppler ultrasonography in obstetrics. *Ultrasound Obstet Gynecol* 2013; **41**: 233–239.
72. Tongsong T, Tongprasert F, Srisupundit K, Luewan S. The complete three-vessel view in prenatal detection of congenital heart defects. *Prenat Diagn* 2010; **30**: 23–29.
73. Yagel S, Cohen SM, Achiron R. Examination of the fetal heart by five short-axis views: a proposed screening method for comprehensive cardiac evaluation. *Ultrasound Obstet Gynecol* 2001; **17**: 367–369.
74. Sheley RC, Nyberg DA, Kapur R. Azygous continuation of the interrupted inferior vena cava: a clue to prenatal diagnosis of the cardiosplenic syndromes. *J Ultrasound Med* 1995; **14**: 381–387.
75. Gonçalves LF, Espinoza J, Romero R, Kusanovic JP, Swope B, Nien JK, Erez O, Soto E, Treadwell MC. Four-dimensional ultrasonography of the fetal heart using a novel Tomographic Ultrasound Imaging display. *J Perinat Med* 2006; **34**: 39–55.

SUPPORTING INFORMATION ON THE INTERNET

Appendix S1, Table S1, Figures S1 and S2 and Videoclips S1–S11 may be found in the online version of this article.

Published 2017. This article is a U.S. Government work and is in the public domain in the USA. *Ultrasound Obstet Gynecol* 2017; **50**: 476–491.
Ultrasound in Obstetrics & Gynecology published by John Wiley & Sons Ltd on behalf of the International Society of Ultrasound in Obstetrics and Gynecology.